JTIP Journal of Trade & Industrial Policies
Vol 01, No. 01,
Spring & Summer 2026

Development of Chitosan/Nanohydroxyapatite particles/$AgNO_3$/ vancomycin scaffold for vancomycin delivery

A.R. Adarangi, Faculty of Mining and Materials, Tarbiat Modares university

S.M.M. Hadavi[1], Faculty of Mining and Materials, Tarbiat Modares university (Corresponding author)

S. Hesaraki, Nanotechnology and Advanced Materials Research Institute

https://doi.org/10.22034/jtip.2026.741522

| Received: 15 May. 2026 | Accepted: 01 September. 2026 |

Abstract

Tissue engineering is defined by some characteristics such as biocompatibility, biodegradability, low immunogenicity, bio absorbability, nontoxicity, rejuvenation, and restoration properties. However, 3D-Scaffold are used having these characteristics with physical and chemical consideration. In this study a three-dimension scaffold was synthesized containing chitosan, Nanohydroxyapatite as an osteoconductive material, AgNO3 as an antiviral as well as anticancer therapeutic agent, and vancomycin that is considered for treating a number of bacterial infections. The behavior of the synthesized scaffold as a drug release material was investigated. Scaffolds were synthesized by freeze drying technique and characterized by scanning electron microscopy (SEM), Fourier transform infra-red spectroscopy, antibiogram method for In vitro tests and UV absorption device for evaluating the drug release behavior. It was found that drug delivery of scaffolds depended on the HA and AgNO3 content whereas less HA resulted in more drug release and AgNO3 postponed the vancomycin release after about 1000 h examination. Moreover, the diagram of drug delivery system demonstrated the predictable release manner of vancomycin in scaffolds. Results of drug delivery tests indicated that AgNO3 have controllable efficacy on sustain delivery and with surpassing percentage of Ag, release of vancomycin have been extended more than 1 month with 60% delivery of drug.

Keywords: Tissue engineering; Drug delivery system; Scaffold; Hydroxyapatite; Chitosan.

چکیده

این پژوهش به سنتز و ارزیابی داربست سه‌بعدی نوین در مهندسی بافت با روش خشک‌کردن انجمادی می‌پردازد که حوزه‌ای پیشران و با ارزش افزوده بالا در صنایع زیست‌پزشکی و بیومواد معدنی به حساب می‌آید. ماتریس این داربست از کیتوسان، ماده رسانای استخوانی نانوهیدروکسی‌آپاتیت (nHA)، نیترات نقره ($AgNO_3$) به‌عنوان عامل ضدسرطان و ضدویروس و داروی وانکومایسین جهت مقابله با عفونت‌های باکتریایی تشکیل شده است. در این مسیر ساختار و کارایی محصول با تکنیک‌های FTIR، SEM، آزمون‌های آنتی‌بیوگرام و طیف‌سنجی UV برای بررسی رفتار رهایش دارو سنجیده شد. از منظر فنی و اقتصادی، نتایج نشان‌دهنده قابلیت بالای تجاری‌سازی فرمولاسیون به‌دلیل دستیابی به رهایش کنترل‌شده و پایدار است؛ عاملی که هزینه‌های مراقبت درمانی و ریسک شکست پیوند را کاهش می‌دهد. غلظت ترکیبات معدنی و دارویی نقشی تعیین‌کننده دارد: کاهش nHA منجر به افزایش شدت رهایش دارو شده، درحالی‌که افزایش $AgNO_3$ آزادسازی وانکومایسین را تعدیل و تا بیش از ۱۰۰۰ ساعت به تأخیر می‌اندازد. در نمونه‌های دارای درصد نقره بالاتر، آزادسازی دارو روندی کاملاً قابل‌پیش‌بینی و پایدار یافته و پس از گذشت بیش از یک ماه به ۶۰ درصد کل بارگیری رسید. تلفیق مواد معدنی فرآوری‌شده (هیدروکسی‌آپاتیت و نقره) با پلیمرهای زیستی، این محصول را به گزینه‌ای رقابتی و استراتژیک در صنایع نوین ترمیم استخوان و سیستم‌های هوشمند رهایش دارو بدل می‌سازد.

1. s.hadavi@modares.ac.ir

1. Introduction

Due to the importance of tissue engineering, scientists highly focused on this filed of science and technology in recent years [Khademhosseini and Langer, 2016]. However, recent research is devoted to bone tissue engineering and in particular to 3D porous scaffold by which specific living cells and drugs are released to a tissue in the period of regeneration or replacement [Langer and Vacanti, 2016]. Clearance of biopharmaceuticals such as nucleic acids, peptides, and amino acid are often confined by feeble stability and quickly out from the body. These challenges, are developed novel drug delivery systems that overcome sustained delivery obstacles with cooperation pharmaceutical sciences. When a pharmaceutical agent is encapsulated within, or attached to, a polymer or lipid, drug safety and efficacy can be greatly improved and new therapies are possible [Langer, 1998].

Despite of the research and improvement of methodologies and materials in the field of polymer drug delivery, still efforts are focused on this subject. Polymer carriers that are accompanied with therapy agents provide adequate condition for temporary controlling and release of a drug by dissolution or degradation of the carrier.

Suitable selection of polymer affects the performance of the drug delivery system, as the polymer influences directly on efficacy and efficiency of the rate and duration of release. On the other hand, some ceramics such as hydroxyapatite (HA) particles has been the subject of interest as a drug carrier due to its osteoconductivity and biocompatibility characteristics [Hoseinzadeh et al., 2016]. No antibacterial activity of HA particles has been reported [Fragal et al., 2016, Kavasi et al., 2017].

Silver ions have been used in medical devices, pharmaceutical products in the treatment of various bacterial infections. Alliance HAp, Ag + has been created the situation to utilize properties of two elements [Liu and Man, 2017]. Sustained drug delivery of vancomycin was depended on the ratio of scaffold materials. In addition, mechanical and physical properties must be considered for creation optimized scaffold.

Drug delivery systems (DDS) have been expanded to enhance bone ingrowth and regeneration in the treatment of bone defects. Researches have been demonstrated the main role of porosity, pore size and interconnected pores in scaffold design and significant effect on tissue engineering and DDS application [Ginebra et al, 2006]. Drug delivery systems have inherent advantages and limitations. Drug release from any carrier is determined by a complex interaction between the drug and polymer in environmental/in vivo conditions. Depending on the drug release behavior, drug delivery devices have been classified into three major classes: diffusion controlled, chemical processes, controlled, and externally or electronically controlled.

Chitosan is a natural polysaccharide and is considered the largest biomaterial after cellulose in terms of distribution and utilization and is significant choice for drug delivery system as scaffold for repair of bone defects, bone marrow-derived, cartilage healing, bone regeneration [Park, 2017]. Chitosan has many physical, chemical and biological properties

referred by its functional groups (amino NH2 and hydroxyl OH). Researchers have utilized a nanoparticle-embedded chitosan sponge for Topical and Local Administration of Chemotherapeutic Agent [Goldberg et al., 2014].

Other researchers investigated the enhancing cell penetration and proliferation in chitosan hydrogels for tissue engineering applications and fabrication of porous chitosan scaffolds for soft tissue engineering [Ji et al., 2011].

In recent years comprehensive studies have been carried on characteristics of chitosan in the drug delivery areas such as antibiotic drug with using chitosan nanoparticles [Zhao et al. 2013], enhance antitumor efficiency by targeted drug delivery via CD44 [Wang et al., 2017]. Hydrophobic–hydrophilic interactions between drug-polymer and drug-release medium may also effect on the release kinetics [Bose and Tarafder, 2012]. Chitosan/nano hydroxyapatite composites have been more application for tissue engineering, because of its ability to impel a good proliferative response in osteoblasts [Lee et al., 2014].

Silver is an appropriate choice for targeting treatment in cancer therapy in drug delivery fields. Silver nanoparticles (AgNPs), as effective antimicrobial agents with low toxicity, have been studied widespread and used in various fields [Sharma et al., 2009]. Chitosan interacts with many metals, including Ag+, Cu2+, Fe3+ and Zn2+. Due to the existence of amine (NH-) and hydroxyl (OH-) groups, the chitosan chains easily bind to the Ag+ , the CH/Ag beads show a smooth and firm surface which becomes smoother with the increase in the AgNPs content because interfacial interactions and intermolecular cross linkers [Freire et al., 2016]. Antimicrobial and anticancer activities have been showed in the porous chitosan-alginate biosynthesized silver nanoparticles, and use of chitosan/silver as a novel carrier [Wakure et al., 2016].

Previous studies in XRD patterns have been indicated that Ag is incorporated within the HA, combination of HAp and Ag+ ions is the best way for ensuring antibacterial achievement with delivery of Ag ions directly to the implant tissue interface [Ciobanu, 2013].

Vancomycin (C66H75Cl2N9O24) have been applied in several applications such as chitosan and calcium sulfate scaffold [Doty et al., 2014]. For more than 4 decades, vancomycin has been the antibiotic of choice for methicillin-resistant Staphylococcus aureus (MRSA) infections. Due to damage to vital organs such as heart and kidneys via systemic administration, VCM is preferred to be used locally special in the form of scaffold. Beginning in the early 1980s, a dramatic increase in vancomycin use occurred, with a >100fold increase occurring over the next 2 decade [Kirst et al., 1998].

The antibacterial activities of composite scaffolds were investigated by a zone inhibition method [Yang et al., 2017]. Scaffold samples were cut in disk shape with 1.5cm in height and 1.4 cm in diameter. Bacillus cereus (B. cereus) ATCC-12228 and staphylococcus aureus (S. aureus) ATCC-47077 as Gram + bacteria and Escherichia coli (E. coli) ATCC-25922 as Gram– were used for antibacterial studies [Numao et al., 1997]. Using the spread plate method, different plates were inoculated with 1 mL of bacterial suspension containing

approximately 10cfu/mL of each bacterium. The scaffolds were placed on the inoculated plates and were incubated at 37°C for 24 hours. Zones of inhibition were distinguished by measuring the clear area formed surrounding each scaffold

2. Materials and Research Procedures

2.1 Reagents and media

Chitosan powder with minimum 85% deacetylated with Mw of 310,000 g/mol, synthetic hydroxyapatite nano-powder with purity of more than 97% purchased form Sigma-Aldrich, acetic acid 96% with a density of 1.06 g/cm3, vancomycin (chemscene) and AgNO3 obtained from Merck were used in this study.

Phosphate buffered saline (PBS) solution was prepared in lab with the following process for 1 liter of PBS: 8 g of NaCl (Merck) together with 0.2 g of KCl (Merck), 1.44 g of Na2HPO4 (Merck) and 0.24 g of KH2PO4 (Merck) was added to 800 ml of distilled water and then the pH was adjusted to 7.4 with HCl (Merck) and distilled water to a total volume of 1 liter. Materials were freeze-dried after which the frozen water is converted directly into the gas phase in sublimation form, which results in pore formation .This method was first utilized by Whang et al. to fabricate PLGA scaffolds [Sachlos and Czernuszka, 2003].

2.2 Preparation of scaffolds

Samples preparation has been carried out in 4 laboratory flasks separately. Three volumetric flasks the samples C1, C2, C3 were prepared according to Table (1) where acetic acid 2% (Merck 96% with a density of 1.06 g/cm3) was used as the solvent. The solutions were homogenized with the aid of magnetic rotator with 3500 rpm for 24 Hours. Control sample (sample C) was prepared without using AgNO3. Then Ag and vancomycin were added to solution in flasks and operation of mixing continued for 48 hours with the same velocity.

HA nanoparticles were added to the solutions and were mixed for 24 hours. Then the mixture was transferred into molds and were kept in freezer at a preset temperature of -50°C to solidify the solvent and induce a solid–liquid phase separation. After 12 hours, the frozen mixture was transferred into a freeze dryer. Scaffolds have kept in -50ºC condition for 3 days. Fig. 1 shows the appearance of the prepared scaffolds.

Table. 1. Ratios of components in the prepared scaffolds (wt%)

Samples	Chitosan	HA	AgNO3	Van	Acid acetic
C1	2.35	0.97	0.04	0.04	96.6
C2	3.00	0.32	0.04	0.04	96.6
C3	1.99	0.97	0.4	0.04	96.6
C	2.39	0.97	0	0.04	96.6

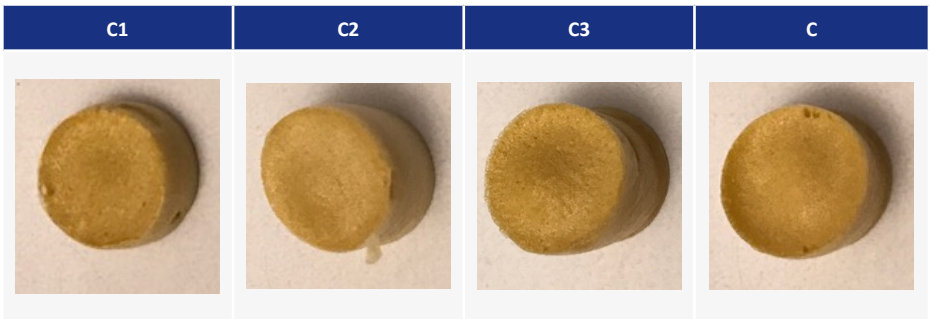

Fig. 1. Prepared samples C1, C2, C3 and C

The morphology and microstructure of the samples before and after examinations were studied using optical (Olympus) and scanning electron microscopy (SEM KYKY EM3200). The compression test was used with Instron (Model: 4505, UK) by applying load via 1 n load cell at a crosshead speed of 2 mm/min in ambient conditions. Fourier transform infrared (FTIR) spectra were obtained using a Nicolet 5-DXB FTIR spectrometer.

X-ray diffraction (XRD) is a versatile analytical method for the detection and quantitative determination of various crystalline phases. XRD data were collected via Philips PW 1710 diffract meter with Cu K□ radiation (□= 1.5406 E) and graphite monochromatic, operated at 45 kV; 30 mA and 25□C.

3. Results and Discussions

3.1 Optical analysis

Increasing the amount of Ag ions in solution change the color of the solution, and hence, the final appearance of dried sample (Fig.1). There is progressively color alternation yellow to brown when ascending Ag ions percentage indicating the change in the structure of Ag when combined with chitosan. As the concentration of silver increases, absorption peak decreases, which might probably be due to the formation of clusters, thereby, decreasing the formation of Ag ions, as described by others [Wei et al., 2009].

3.2 SEM specification

The surface morphologies of all of the scaffolds were studied by scanning electron microscopy. The pores and interconnectivity of porosities are evident from SEM images in Fig. 2. Examinations show that the pores in sample C1 were symmetrical and relatively uniform, whereas in C2 and C3 samples, pores were irregular in shape and bigger. C1 sample possesses HA three times of C2 whereas C3 possesses AgNO3 ten times of C1. Fig. 2 also shows that interconnectivity of the pores is obtained which is important for scaffolds for cell growth and vascularization.

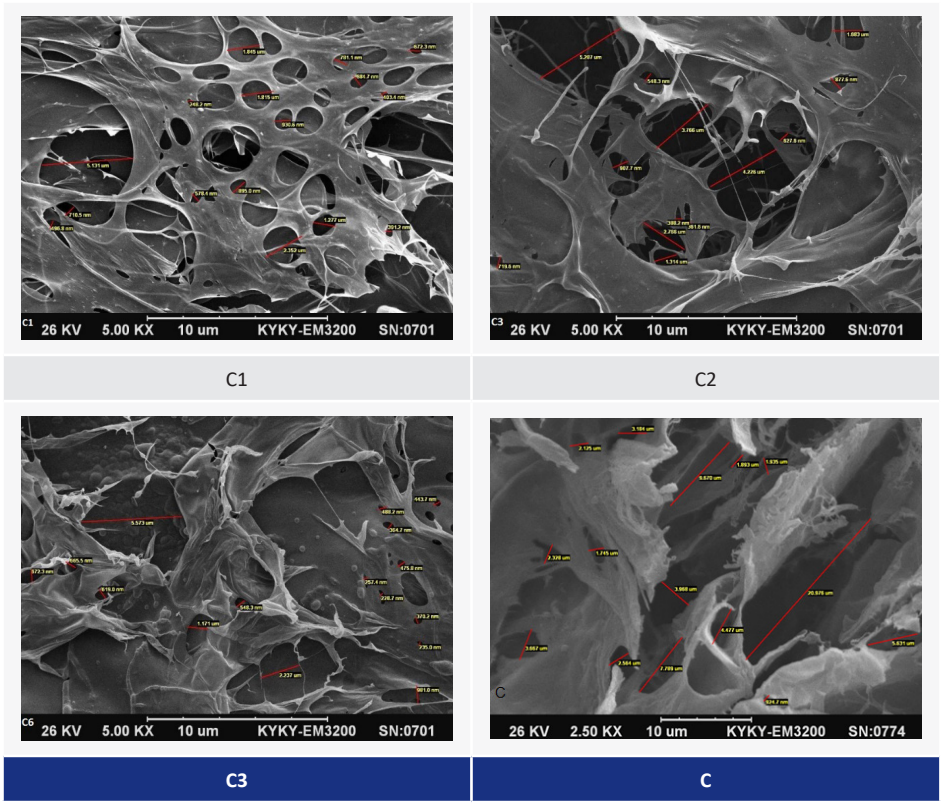

Fig. 2. Scanning electron microscopy images of prepared scaffolds.

The effect of pore size and structure is reviewed by others [Huang et al, 2025]. The porosity of the scaffolds was calculated by measuring their dimension and weight. The average pore size was calculated from scanning electron microscopy images. A typical porosity of 70% in addition a pore diameter of at least 100 µm is known to be compulsory for cell penetration and a proper vascularization of the ingrown tissue [Ramay, Zhang, 2004].

The total porosity (P) of scaffolds can be determined by measuring the porosity and scaffold volume. For measuring the porosity volume, the scaffold was immersed in ethanol alcohol and the absorbed weight was recorded:

$$v_{porosity} = \frac{mass\ of\ absorbed\ alcohol}{\rho_{ethanol\ alcohol}} \quad (1)$$

$$Total\ posority = \frac{v_{porosity}}{v_{scaffold}} \quad (2)$$

Where ρ scaffold is 0.789 g/cm^3. The volume of scaffold is calculated by measuring the diameter and height of the sample. The result is shown in Table (2).

Table. 2. Porosity percent in scaffolds studied

	C1	C2	C3	C
Diameter of the samples (mm)	27.96	28.2	28.6	28.04
Average height of the samples (mm)	3.7	5.17	5.1	5.18
Volume of scaffold (cm^3)	2.272	3.232	3.275	3.202
Weight of alcohol absorbed (gr)	1.36	2.06	2.01	1.79
Volume of pores (cm3)	1.72	2.61	2.55	2.27
ΔV/V	76%	81%	78%	71%

Table 2 shows that increasing in HA percent caused decreasing porosity from 81% to 76%. Moreover, results showed increasing AgNO3 in C3 sample enhancing porosity from 76% to 78%. Comparison between C and C1 samples indicates that AgNO3 (0.04%) is caused to increasing porosity 71% to 76%.

In other words, pore average size and interconnected porosity in SEM images have shown that pores with 250 to 500 nm in sample C1 was changed with chitosan and AgNO3 percentage. As AgNO3 increased in C3 sample in comparison with that of C1 sample, pores size was decreased with ease of their interconnection. Moreover, comparison between C1 and C sample showed that presence of AgNO3 in scaffold would affect pore size and their interconnection.

3.3 Mechanical analysis

Compressive strength is an important mechanical parameter for porous scaffolds. Therefore, a mechanical test was performed to find out the compressive strength of the prepared scaffolds. The stress–strain curve obtained was used to determine the mechanical properties. Fig. 3 shows the results of the mechanical tests on the prepared scaffolds.

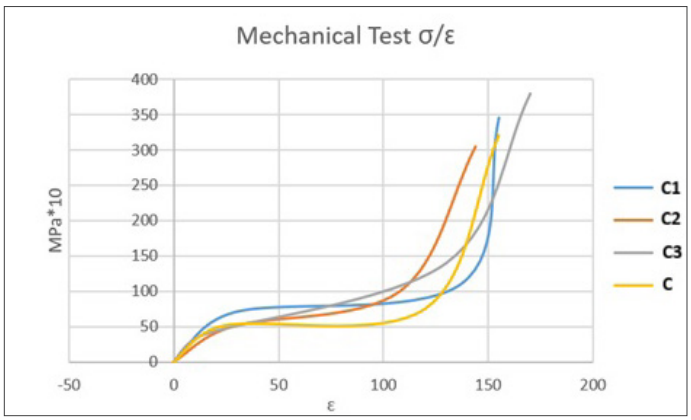

Fig. 3. Stress-strain curves of the scaffold samples.

As demonstrated in Fig. 3 maximum compressive strength for C1, C2, C3 and C was found as 10.2, 7.6, 12.2 and 5.5 MPa, respectively. The highest amount in C3 sample shows the effect of AgNO3 and HA on increasing the compressive strength. The strength of control sample without AgNO3 was less than those of C1 and C3 sample and higher than that of C2 scaffold. This shows the effect of HA as C sample possess about three times of that in C2 sample. A similar founding was reported by other researchers showing that increasing the HA led to an increase in the compressive strength. The incorporation of chitosan into scaffold resulted in decreasing of compressive strength due to the weaker interfacial bonding between chitosan and HA matrix. Li et al. compared the compressive strengths of dense scaffolds with different Chitosan/HA composite ratio and reported the maximum compressive strength to be 119.86 MPa at the chitosan/HA ratio of 30:70 [Li et al., 2005].

3.4 FTIR Spectroscopy analysis

A small amount of powder was scratched from the surface of the scaffolds, milled with KBr, and pressed into a transparent disk for analysis. FTIR spectra were gathered at a resolution of 4cm-1 and 256 scans over a range of 400 to 4000 wave numbers (cm-1), according to the reference [Liu et al., 2012].

The FTIR spectral analysis of pure chitosan shows common bands at 3436 cm-1, 2912 cm-1, 1648 cm-1, 1377 cm-1 and 1076 cm-1 that belong to the stretching vibration of OH and NH groups, CH group, amide group, COO group of carboxylic acid salt and stretching vibration of C O C in glucose unit. The FTIR spectral analysis of hydroxyapatite powder was showed 3568, 1461, 1041,570 cm-1 that were related to O-H, CO3, PO4 and Hpo4 bonds, according to the references [Lin et al., 2017, Rehman and Bonfield, 1997]. Spectral analysis of AgNO3 was illustrated 3333,1370,1029,1629 cm-1 that were reported by other research [Popovych et al., 2016, Han et al., 1998]. Some feeble pick in the range of 1000 to 1750 were occurred that related to the vancomycin in the scaffolds (Fig. 4).

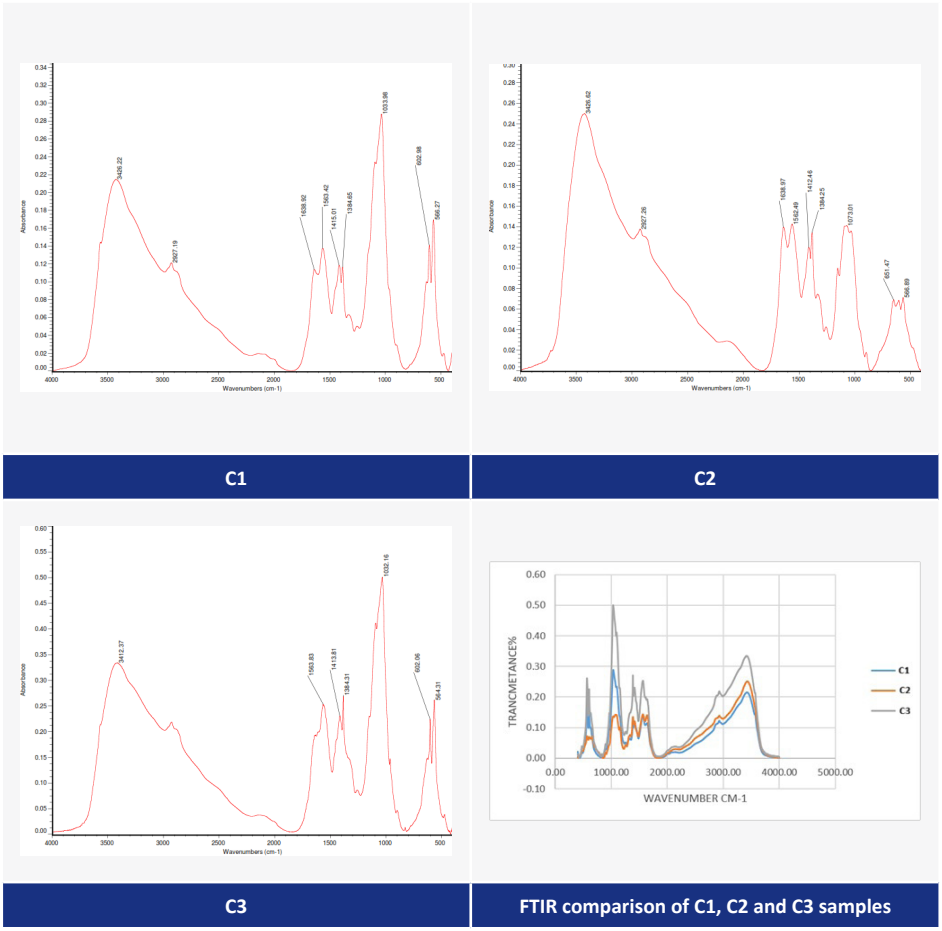

Fig. 4. FTIR results of prepared scaffolds in this study

The peaks in the range of 3000 to 3500 cm-1 represented the O-H and N-H bond that was related to HA and chitosan. In the region of 2500 to 3000 cm-1 the peak at 2927 cm-1 was related to the C-H bond in chitosan. In the range of 1000 to 1500 cm-1 the PO4 peak was detected with different intensity in C1 and C3 samples. The 566 cm-1 peak was HPO4 in all samples. The 1415 cm-1 peak was related to C-N bond that was demonstrated in all samples. N-H bond in chitosan was showed at 1638 cm-1.

3.5 XRD Analysis

The structural properties of chitosan-Ag composites were analyzed using XRD technique. Peaks of chitosan was at 2θº of 10.5,20,22, and those of Ag at 9, 38.18, and 44.25. Hydroxyapatite was exhibited some peaks at 26, 31.5, 32.5, 33, 40, 47, 50, 54 (Fig. 5). Sharp peak at 2θ of 9º relates to AgNO3 which shows relatively high amount of this phase in sample C3. With decreasing HA in C2 sample, intensity of peaks and also crystallinity were

reduced.

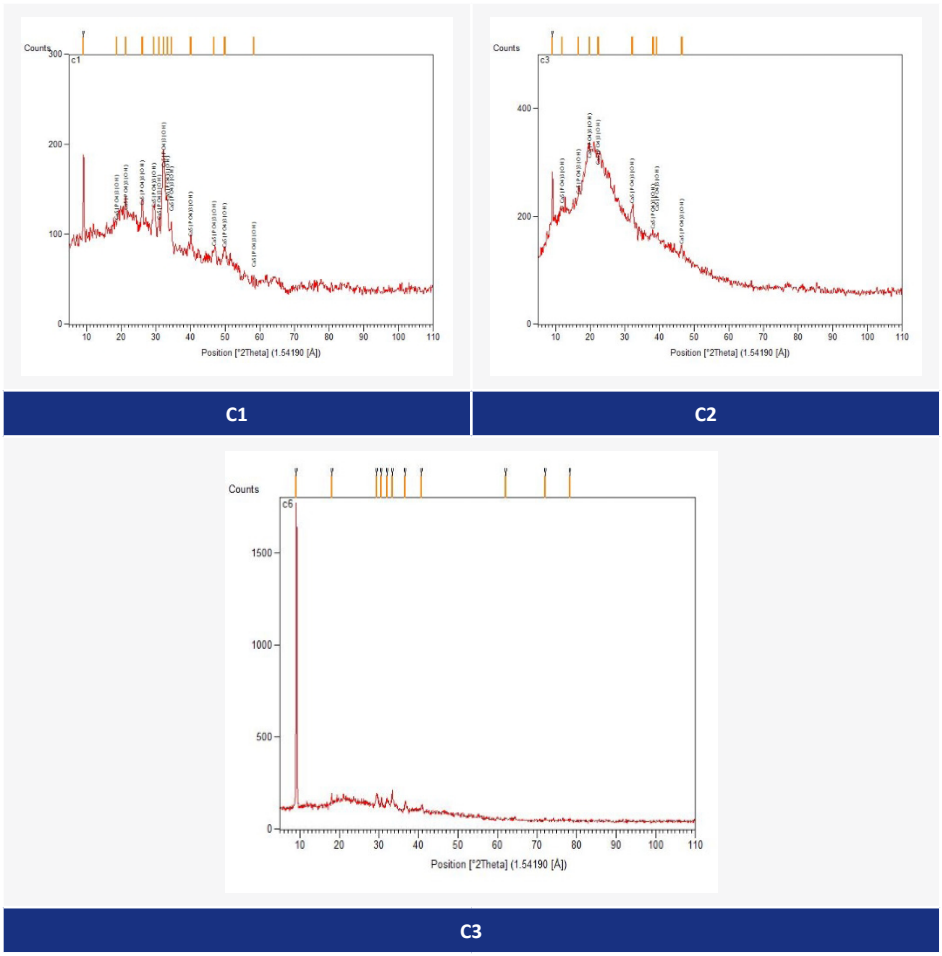

Fig. 5. XRD patterns of prepared scaffolds

3.6 Antibacterial Activity of scaffolds

The antibacterial activities of composite scaffolds were investigated by a zone inhibition method. Fig. 6 shows the appearance of the scaffolds after exposure to different bacteria.

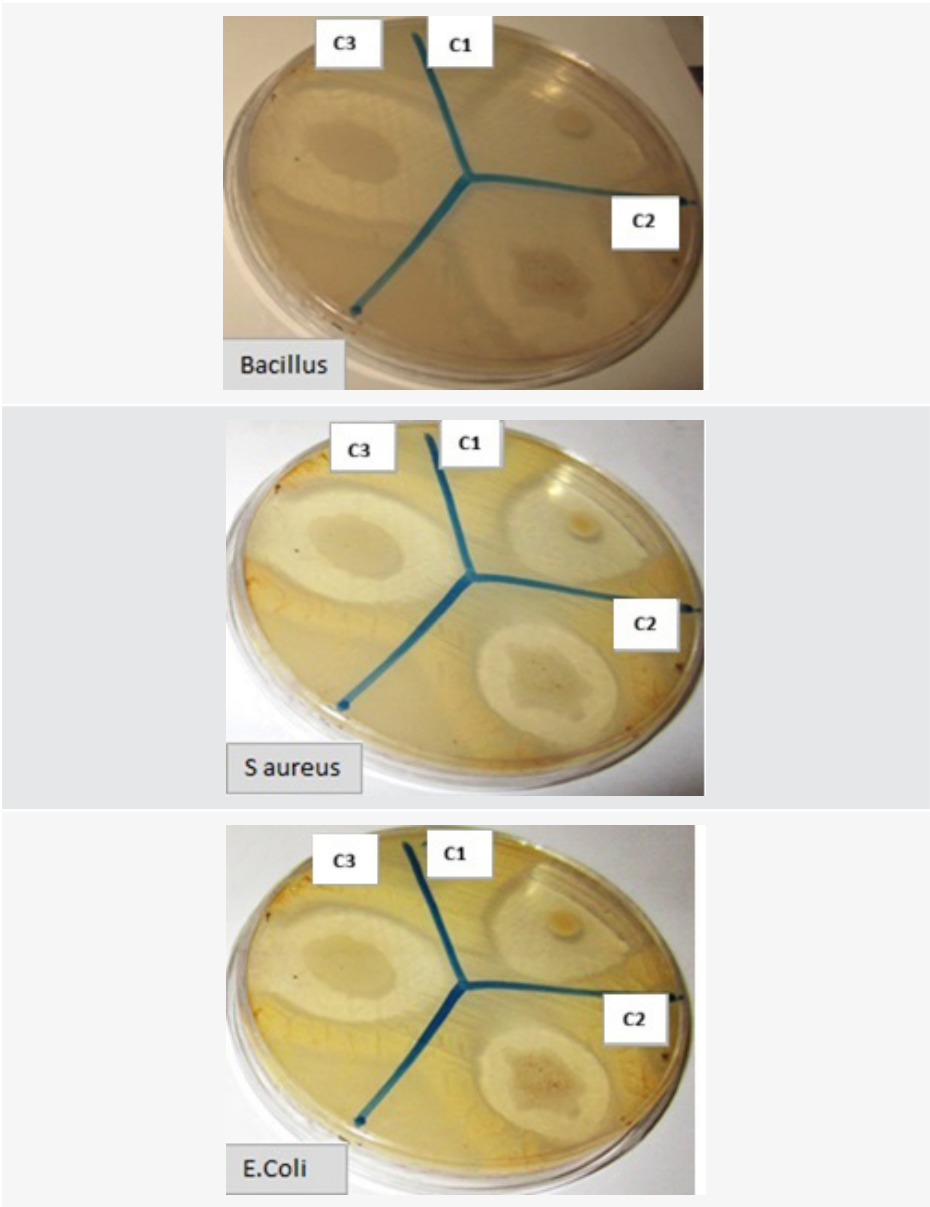

Fig. 6. Antibacterial analysis of the studied scaffolds samples

Diameter of inhibition of each scaffolds against Basillus, S aureus and E. Coli were determined and results are shown in Table 3.

Table. 3. Diameter of inhibition in antibacterial analysis (mm)

	Bacillus	S aureus	E.Coli
C1	11.3± 1.3	9.4± 1.3	8.5± 1.3
C2	7.8± 1.1	6.2± 1.4	5.9± 1.4
C3	16.7±2.5	14.5± 1.5	13.7± 1.3

Inhibition activity of scaffold samples against three different bacteria is such that C3 possesses largest diameter whereas C2 showed least diameter. Regardless of the bacteria type, increasing AgNO3 and reducing HA resulted in more antibacterial activity.

3.7 Swelling characteristics of the scaffolds

Prior to inserting in phosphate buffered saline (PBS), the weight of each scaffolds sample was recorded as *W0*. Then, the scaffolds were immersed in the prepared PBS with pH of 7.4, at 37ºC for 24 hours. After 24 h, the scaffolds were taken out of PBS, cleansed, dried and weighed. The obtained weights of the scaffolds were recorded as *Ww*. The ratio of swelling was determined using the following equation:

$$Swelling\ ratio = {(W_w - W_0)}/{W_0}$$

Fig. 7 shows the swelling ratios of scaffold samples, which are 26, 53, 32 and 24 for C1, C2, C3 and C, respectively. From the results, it is clear that increasing AgNO3 in C3 increased the adsorption in comparison with those of C1and C samples. Moreover, reduction of HA in sample C2 increased the adsorption and hence, swelling ratio.

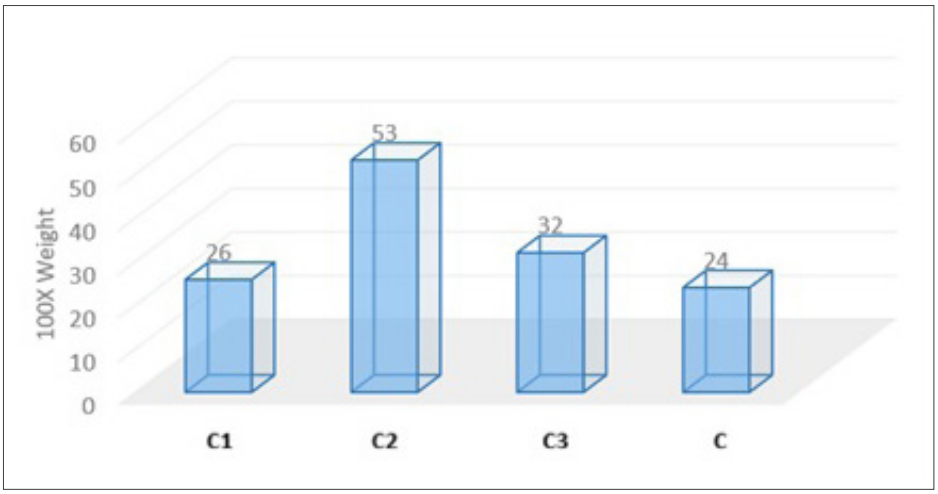

Fig. 7. Percent of PBS adsorption after 24 hours

3.8 Determination Drug release

After taking out scaffolds from freeze dryer device, the samples were prepared for drug release experiments. This test is indeed the diffusion test of drug from the scaffold. Uniform section of scaffolds was prepared and put in falcon tubes with 20 ml of phosphate buffered saline (PBS) with pH of 7.4 in a water bath at 37□C. The drug molecules entrapped in the scaffold were released in period of time in PBS environment. In interval of time of 1h, 3h, 8h the samples were taken out of falcon tube. By using UV absorption device, the amount of released drug was determined.

In order to quantify drug release, various mathematical models are proposed and used [Martнn-Camacho et al., 2023, Azadi et al., 2017, Gomes-Filho et al., 2019]. The Weibull equation can be applied to almost all kinds of dissolutions [Hirai et al., 2017]. In the case of pharmaceutical dissolution, this equation represent the mass of fraction of drug in solution and is given by [Wang et al., 2015]:

$$M = M_o \left[1 - e^{(t - T/a)b}\right]$$

Where, M is the amount of drug dissolved as a function of time t, T accounts for the lag time measured as a result of the dissolution process, parameter 'a' denotes a scale parameter that describes the time dependence. While 'b' describes the shape of the dissolution curve advancement it is equal to 1 where the shape of the curve is similar exactly to the shape of an exponential profile.

Results of vancomycin release from the studied scaffolds are given in Fig. 8. As it is clear from figure, illustrated that with increasing AgNO3 in C3 sample, stability and sustainability of delivery enhanced, such that after 1000 hours, only 42% of drug was released in C3 sample whereas in C2 sample 60% of vancomycin was released. In comparison between C1 and C2 it is was found that less HA in scaffold resulted in higher drug release from about 50% in C1 to 60% in C2 after 1000 hours.

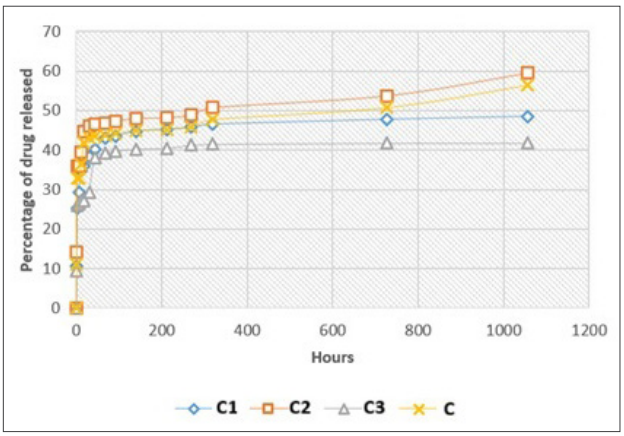

Fig. 8. Release of vancomycin from studied scaffolds.

Conclusions

- The incorporation of chitosan into scaffold resulted in decreasing compressive strength due to the weaker interfacial bonding between chitosan and HA matrix.
- Regardless of the bacteria type, increasing AgNO3 and reducing HA resulted in more antibacterial activity.
- As AgNO3 increased pores size was decreased with ease of their interconnection. Moreover, presence of AgNO3 in scaffold affects pore size and their interconnection.
- Increasing AgNO3 and reduction of Hydroxyapatite increased the adsorption and hence, swelling ratio.
- With increasing AgNO3, stability and sustainability of delivery enhanced, such that after 1000 hours, only 42% of drug was released in C3 sample whereas in C2 sample 60% of vancomycin was released. less HA in scaffold resulted in higher drug release.

References

- Azadi S., Ashrafi H., Azadi A., "Mathematical modeling of drug release from swellable polymeric nanoparticles", Journal of Applied Pharmaceutical Science Vol. 7 (04), pp. 125-133, April, 2017, DOI: 10.7324/JAPS.2017.70418.
- Bose S, Tarafder S. Calcium phosphate ceramic systems in growth factor and drug delivery for bone tissue engineering: a review. Acta biomaterialia. 2012;8(4):1401-21.
- Ciobanu CS, Iconaru SL, Pasuk I, Vasile BS, Lupu AR, Hermenean A, et al. Structural properties of silver doped hydroxyapatite and their biocompatibility. Materials science & engineering C, Materials for biological applications. 2013;33(3):1395-402.
- Doty HA, Leedy MR, Courtney HS, Haggard WO, Bumgardner JD. Composite chitosan and calcium sulfate scaffold for dual delivery of vancomycin and recombinant human bone morphogenetic protein-2. Journal of materials science Materials in medicine. 2014;25(6):1449-59.
- Hoseinzadeh S, Atashi A, Soleimani M, Alizadeh E, Zarghami N. MiR-221-inhibited adipose tissue-derived mesenchymal stem cells bioengineered in a nano-hydroxy apatite scaffold. In Vitro Cell Dev Biol Anim. 2016;52(4):479-87.
- Fragal EH, Cellet TS, Fragal VH, Companhoni MV, Ueda-Nakamura T, Muniz EC, et al. Hybrid materials for bone tissue engineering from biomimetic growth of hydroxiapatite on cellulose nanowhiskers. Carbohydrate polymers. 2016;152:734-46.
- Freire PL, Albuquerque AJ, Farias IA, da Silva TG, Aguiar JS, Galembeck A, et al. Antimicrobial and cytotoxicity evaluation of colloidal chitosan - silver nanoparticles - fluoride nanocomposites. International journal of biological macromolecules. 2016;93(Pt A):896-903.
- Ginebra MP, Traykova T, Planell JA. Calcium phosphate cements: competitive drug carriers for the musculoskeletal system? Biomaterials. 2006;27(10):2171-7.
- Goldberg M, Manzi A, Aydin E, Singh G, Khoshkenar P, Birdi A, et al. Development of a Nanoparticle-Embedded Chitosan Sponge for Topical and Local Administration of Chemotherapeutic Agents. J Nanotechnol Eng Med. 2014;5(4):0409051-4090511.
- Gomes-Filho M. S., Alves Barbosa M. A., Oliveira F. A., "A statistical mechanical model for drug release: Relations between release parameters and porosity", Physica A: Statistical Mechanics and its Applications, Volume 540, 2020, 123165, doi.org/10.1016/j.physa.2019.123165.
- Han SW, Kim Y, Kim K. Dodecanethiol-Derivatized Au/Ag Bimetallic Nanoparticles: TEM, UV/VIS, XPS, and FTIR Analysis. Journal of colloid and interface science. 1998;208(1):272-8.
- Hirai D, Iwao Y, Kimura SI, Noguchi S, Itai S. Mathematical model to analyze the dissolution behavior of metastable crystals or amorphous drug accompanied with a solid-liquid interface reaction. International journal of pharmaceutics. 2017;522(1-2):58-65.
- Huang, D., Li, Z., Li G., Zhou F., Wang G., Ren X., Su J., Biomimetic structural design in 3D-printed scaffolds for bone tissue engineering, Materials Today Bio, 32, 2025, 101664, doi.org/10.1016/j.mtbio.2025.101664.
- Ji C, Annabi N, Khademhosseini A, Dehghani F. Fabrication of porous chitosan scaffolds for soft tissue engineering using dense gas CO2. Acta biomaterialia. 2011;7(4):1653-64.
- Kavasi RM, Berdiaki A, Spyridaki I, Corsini E, Tsatsakis A, Tzanakakis G, et al. HA metabolism in skin homeostasis and inflammatory disease. Food Chem Toxicol. 2017;101:128-138.
- Khademhosseini A, Langer R. A decade of progress in tissue engineering. Nature protocols. 2016;11(10):1775-81.
- Kirst HA, Thompson DG, Nicas TI. Historical yearly usage of vancomycin. Antimicrobial agents and chemotherapy. 1998;42(5):1303-4.
- Langer R. Drug delivery and targeting. Nature. 1998;392(6679 Suppl):5-10.
- Langer R, Vacanti J. Advances in tissue engineering. J Pediatr Surg. 2016;51(1):8-12.
- Lee JS, Baek SD, Venkatesan J, Bhatnagar I, Chang HK, Kim HT, et al. In vivo study of chitosan-natural nano hydroxyapatite scaffolds for bone tissue regeneration. International journal of biological macromolecules. 2014;67:360-6.
- Li Z, Yubao L, Aiping Y, Xuelin P, Xuejiang W, Xiang Z. Preparation and in vitro investigation of chitosan/nano-hydroxyapatite composite used as bone substitute materials. Journal of materials science Materials in medicine. 2005;16(3):213-219.
- Lin Z, Hu R, Zhou J, Ye Y, Xu Z, Lin C. A further insight into the adsorption mechanism of protein on hydroxyapatite by FTIR-ATR spectrometry. Spectrochimica acta Part A, Molecular and biomolecular spectroscopy. 2017;173:527-31.
- Liu BW, Zhao HH, Zhao P, Wang W, Xue HQ, Wang YH, et al. [The FTIR spectral characteristics and comparison study of Astragalus menbranceus soil]. Guang pu xue yu guang pu fen xi = Guang pu. 2012;32(11):2981-6.

- Liu X, Man HC. Laser fabrication of Ag-HA nanocomposites on Ti6Al4V implant for enhancing bioactivity and antibacterial capability. Materials science & engineering C, Materials for biological applications. 2017;70(Pt 1):1-8.
- Martín-Camacho U.J., Rodríguez-Barajas N., Sánchez-Burgos J. A., Pérez-Larios A., "Weibull β value for the discernment of drug release mechanism of PLGA particles", International Journal of Pharmaceutics, Volume 640, 2023, 123017. doi.org/10.1016/j.ijpharm.2023.123017.
- Numao N, Iwahori A, Hirota Y, Sasatsu M, Kondo I, Onimura K, Antibacterial activity of two alkylamines integrated an indane scaffold: mimicry of a complementary unit on magainin 2. Biol Pharm Bull. 1997;20(7):800-4.
- Park K. Chitosan-gelatin-platelet gel composite scaffold for bone regeneration. Journal of controlled release : official journal of the Controlled Release Society. 2017;254:137.
- Popovych N, Kyriienko P, Soloviev S, Baran R, Millot Y, Dzwigaj S. Identification of the silver state in the framework of Ag-containing zeolite by XRD, FTIR, photoluminescence, (109)Ag NMR, EPR, DR UV-vis, TEM and XPS investigations. Physical chemistry chemical physics : PCCP. 2016;18(42):29458-65.
- Ramay HR, Zhang M. Biphasic calcium phosphate nanocomposite porous scaffolds for load-bearing bone tissue engineering. Biomaterials. 2004;25(21):5171-80.
- Rehman I, Bonfield W. Characterization of hydroxyapatite and carbonated apatite by photo acoustic FTIR spectroscopy. Journal of materials science Materials in medicine. 1997;8(1):1-4.
- Sachlos E, Czernuszka JT. Making tissue engineering scaffolds work. Review: the application of solid freeform fabrication technology to the production of tissue engineering scaffolds. Eur Cell Mater. 2003;5:29-39; discussion -40.
- Sharma VK, Yngard RA, Lin Y. Silver nanoparticles: green synthesis and their antimicrobial activities. Adv Colloid Interface Sci. 2009;145(1-2):83-96.
- Wakure BS, Bhatia NM, Syed HB. Noninvasive cellular internalization of silver molecules by chitosan nanoneedles: a novel nanocarrier. J Biomol Struct Dyn. 2016;34(5):971-82.
- Wang M, Zhao T, Liu Y, Wang Q, Xing S, Li L, Ursolic acid liposomes with chitosan modification: Promising antitumor drug delivery and efficacy. Materials science & engineering C, Materials for biological applications. 2017;71:1231-40.
- Wang Y, Abrahamsson B, Lindfors L, Brasseur JG. Analysis of Diffusion-Controlled Dissolution from Polydisperse Collections of Drug Particles with an Assessed Mathematical Model. Journal of pharmaceutical sciences. 2015;104(9):2998-3017.
- Wei D, Sun W, Qian W, Ye Y, Ma X. The synthesis of chitosan-based silver nanoparticles and their antibacterial activity. Carbohydr Res. 2009;344(17):2375-82.
- Yang R, Zhang G, Zhang F, Li Z, Huang C. Membrane Permeabilization Design of Antimicrobial Peptides Based on Chikungunya Fusion Domain Scaffold and Its Antibacterial Activity against Gram-positive Streptococcus Pneumoniae in Respiratory Infection. Biochimie. 2017.
- Zhao L, Zhu B, Jia Y, Hou W, Su C. Preparation of biocompatible carboxymethyl chitosan nanoparticles for delivery of antibiotic drug. Biomed Res Int. 2013;2013:236469.